

Modeling the impact of elastic bodies taking into account dry positional friction and the coefficient of velocity restoration

Oleksiy Bohomolov¹, Oleksiy Zavhorodnii², Petro Hurskyi¹,
Vadym Bredykhin³, Oleksandr Bohomolov¹, Taras Shchur^{4*},
Patrycja Walichnowska⁵ , Weronika Kruszelnicka⁵, Andrzej Tomporowski⁵

¹ Department of Equipment and Engineering of Processing and Food Production, State Biotechnological University, Kharkiv, Ukraine

² Department of Physics and Mathematics, State Biotechnological University, Kharkiv, Ukraine

³ Department of Reliability and Durability of Machines and Structures Named After V.Ya. Anilovich, State Biotechnological University, Kharkiv, Ukraine

⁴ Department of Agricultural Engineering State Biotechnological University, Kharkiv, Ukraine

⁵ Department of Renewable Energy Sources Engineering and Technical Systems, Faculty of Mechanical Engineering, Bydgoszcz University of Science and Technology, Al. Prof. S. Kaliskiego 7, 85-796 Bydgoszcz, Poland

* Corresponding author's e-mail: shchurtg@gmail.com

ABSTRACT

Considering dry positional friction in the model of collinear elastic impact, the stiffness of the system during compression is greater than its stiffness during decompression. The coefficients of the relative motion equation of the bodies involved in the impact have different values at these stages. They depend not only on the geometry of the bodies in the interaction region and the mechanical properties of their materials, but also on the velocity restitution coefficient, which is one of the input parameters of the model, determined a priori through experiments. In the case of power-law nonlinearities in the stiffness of the dynamic system, which corresponds to the solutions of the contact problem in the theory of elasticity, the equation of relative motion of the bodies has closed analytical solutions. During the compression phase, the solution is expressed with an Ateb-sine and its powers, while during the decompression phase, it is expressed with an Ateb-cosine and its powers. To simplify the numerical implementation of the solutions, an approximation of these special functions by trigonometric functions is proposed. This approximation ensures a calculation accuracy of three significant digits after the decimal point. Examples of calculations are provided, demonstrating that accounting for positional friction leads to a decrease in the maximum compression of the bodies, an increase in the peak impact force, and an extension of its duration over time. Variations of impacts between bodies with surfaces of second- and fourth-order in the dynamic interaction region are calculated. The model has much in common with the classical model, but additionally considers the actual value of the velocity restitution coefficient, which is less than one, in collinear impacts. The presented theory applies only to elastic impacts with low initial collision velocities, where no plastic deformations occur.

Keywords: quasi-static collinear impact, elastic bodies, positional friction, analytical solution, periodic Ateb-functions.

INTRODUCTION

The impact of solid bodies is a rapid mechanical process. Despite its short duration, significant forces of dynamic interaction arise during an impact, which can lead to the

destruction of structural elements, particularly those made from brittle materials. This creates a challenge in ensuring the strength of airplane glass when colliding with birds in mid-air, as well as the durability of the coverings and glass of other vehicles. Similarly, impacts from hail

can damage fruits and vegetables, posing a problem that requires appropriate calculations. Such calculations are also necessary in cases where mechanical impact plays a key role in technological processes, such as forging in mechanical engineering, driving piles in construction, using jackhammers in mining, etc. Additionally, mechanical impact is involved in certain methods of separating seed mixtures in agricultural production. Thus, mechanical impact frequently occurs in human activities, and its modeling is an important scientific and applied problem.

There are several variants of impact theory [1, 2]. The first to emerge historically was the stereomechanical theory, which is based on general mechanical theorems and energy principles. An important physical characteristic in this theory is the velocity restitution coefficient, which is often used in calculations. However, stereomechanical theory does not allow for determining the duration of the impact or the force of the impact interaction, as it assumes the impact to be instantaneous and replaces the concept of force with its impulse. A second variant is the wave theory of impact, which studies the propagation of elastic and elastoplastic waves in bodies subjected to impact. Determining the impact force and its duration became possible with the advent of the quasi-static theory, which assumes that during the impact, waves travel several times the distance characterizing the size of the body. A hybrid version of the theory, combining quasi-static and wave theories of impact, has found wide practical application [3, 4].

The second common approach to improving impact theories involves replacing elastic bodies with viscoelastic ones. This model was initiated in [5] and explored with certain variations in [6–8]. In this model, the velocity restitution coefficient depends on the initial impact velocity, which is confirmed in practice [9, 10], where it decreases as the collision velocity increases.

The third direction of modifying the classical theory involves accounting for hysteresis energy losses during the dynamic deformation of bodies [11]. In such models, the velocity restitution coefficient is less than one, but it does not depend on the impact velocity, which is a certain drawback of the model.

The fourth direction is related to the consideration of dry friction [12, 13], which can be regarded as positional friction, as the value of the friction force depends on the displacement of the bodies. Despite its drawbacks, this model is relatively simple, and with proper identification of the coefficients, it can provide adequate results. We will further develop this direction, but unlike the general solution of the problem in quadratures [14], we will construct a closed analytical solution, limiting ourselves to a class of power-law nonlinearities that correspond to the theory of contact deformations of elastic bodies [15]. This solution is expressed through periodic Ateb functions, which have gained popularity in the theory of nonlinear oscillations [16–19], and recently in the theory of mechanical impacts [20, 21]. Due to the availability of compact approximations of these special functions, there are no difficulties in the numerical implementation of the analytical solution.

The goal of this paper is to develop a mathematical model of a dissipative collinear impact of elastic bodies with positional friction, which considers the results of experimental determination of the velocity restitution coefficient. It should be noted that determining this coefficient is one of the simplest tasks when measuring the parameters of a transient mechanical process.

MATHEMATICAL MODELS

The proposed model considers the dependence of the velocity restitution coefficient on the initial impact velocity, which enhances the adequacy of the modernized theory compared to its classical version. To achieve these aim, the following tasks have been outlined:

- Mathematical modeling of the dynamic compression of bodies.
- Mathematical modeling of the dynamic decompression of bodies.
- Performing calculations and conducting a comparative analysis of numerical results.

The modeling is based on the theory of nonlinear differential equations, the construction of their exact analytical solutions using special functions, and the approximation of these special functions by elementary functions.

Mathematical modeling of dynamic compression of bodies

In accordance with the quasi-static theory of impact, this process is described by the following differential equation:

$$M\ddot{x} + c_1 x^\alpha = 0, \tag{1}$$

where: $M = \frac{m_1 m_2}{m_1 + m_2}$, m_1, m_2 – the masses of the bodies involved in the impact; $x = x(t)$ – the

approach of the bodies' centers of mass as a function of time t ; $c_1 = c + \Delta c$, $c > 0$, $\alpha > 0$ – constants that depend on the materials of the bodies and the shape of the boundary surfaces in the contact region, in accordance with the solution to the contact problem in elasticity theory [22]; $\Delta c > 0$ – positional friction constant; A dot above a variable x denotes its derivative with respect to t .

Let's assume that the velocity restitution coefficient K is determined experimentally. Then, Δc can be easily calculated using the following formula:

$$\Delta c = \frac{1 - K^2}{1 + K^2} c.$$

Assuming that the collision of the bodies occurs at velocity v_0 , Equation 1 is supplemented with the initial conditions:

$$x(0) = 0; \dot{x}(0) = v_0 \tag{2}$$

To obtain the analytical solution of the problem given by expressions (1) and (2), we rewrite Equation 1 as:

$$\ddot{x} dt = -\frac{c_1}{M} x^\alpha \dot{x} dt.$$

Next, we write it in a form convenient for integration:

$$d\left(\frac{\dot{x}^2}{2}\right) = -\frac{c_1}{M} dx.$$

By integrating, we find, up to a constant c :

$$\dot{x}^2 = c - \frac{2c_1}{M} \cdot \frac{x^{\alpha+1}}{\alpha+1}.$$

Taking into account the initial conditions (2), we determine the unknown constant c which equals v_0^2 . Thus:

$$\dot{x} = \frac{dx}{dt} = v_0 \cdot \sqrt{1 - \frac{2c_1}{Mv_0^2} \cdot \frac{x^{\alpha+1}}{\alpha+1}}.$$

At the point of maximum compression $x = x_c$, the relative velocity of the bodies $\dot{x} = 0$. Therefore, from the last formula, it follows that:

$$x_c = \left[\frac{Mv_0^2}{2c_1} (\alpha + 1) \right]^{\frac{1}{\alpha+1}}$$

This is the expression for the maximum compression of the bodies during impact. By further integrating the velocity x , we obtain:

$$\int_0^x \frac{dy}{\sqrt{1 - \frac{2c}{Mv_0^2} \frac{y^{\alpha+1}}{\alpha+1}}} = v_0 t.$$

By switching to a new integration variable $u = \frac{y}{x_c}$, we reduce the second integral of Equation 1 to the following form:

$$\int_0^{x/x_c} \frac{du}{\sqrt{1-u^{\alpha+1}}} = \frac{v_0 t}{x_c}.$$

Its left side represents the integral form of the Ateb-sine function [20, 23, 24]. Therefore, the analytical solution of Equation 1, considering the initial conditions (2), is expressed through this special function and is as follows:

$$x(t) = x_c Sa\left(\alpha, 1; \frac{1+\alpha}{2} \cdot \frac{v_0 t}{x_c}\right) \tag{3}$$

where: $x_c = \left(\frac{Mv_a^2}{2} \cdot \frac{a+1}{c_1}\right)^{\frac{1}{a+1}}$ is the maximum approach of the centers of mass achieved at the end of the compression process $t = t_a$.

Duration of the compression process t_c , at the end of which $x = x_c$, is equal:

$$t_c = \frac{Ix_c}{v_0}, \tag{4}$$

where

$$I = \int_0^1 \frac{du}{\sqrt{1-u^{\alpha+1}}} = \frac{\sqrt{\pi}}{a+1} \cdot \frac{G\left(\frac{1}{a+1}\right)}{G\left(\frac{a+3}{2a+2}\right)}, \tag{5}$$

where: $G(z)$ is gamma functions, tabulated in [25, 26].

To calculate the body compression forces $P(t)$, we have the formula:

$$P(t) = c_1 x^\alpha = P_c \left[Sa\left(\alpha, 1; \frac{1+\alpha}{2} \cdot \frac{v_0 t}{x_c}\right) \right]^\alpha, \tag{6}$$

where: $P_c = c_1 x_c^\alpha = c_1^{\frac{1}{1+\alpha}} \left[\frac{Mv_0^2}{2} (\alpha+1) \right]^{\frac{\alpha}{\alpha+1}}$ is maximum value of the force $P_c = P(t_c)$.

Mathematical modeling of dynamic decompression of bodies

It occurs on an interval $t \in (t_c; t_y)$ and is described by the differential equation:

$$M\ddot{x} + c_2 x^a = 0, \tag{7}$$

where: $c_2 = c - \Delta c$.

Initial conditions for (7) are:

$$x(t_c) = x_c; \dot{x}(t_c) = 0 \tag{8}$$

The Cauchy problem given by expressions (7) and (8) was also considered in [23], and differs from the one previously solved by the initial conditions. Therefore, it is necessary to construct its analytical solution anew. The first integral of Equation 7, considering conditions (8), has the form:

$$x = \frac{dx}{dt} = \sqrt{\frac{2c_2}{M(a+1)}} \cdot \sqrt{x_c^{a+1} - x^{a+1}}$$

Its second integral is:

$$\int_{x_c}^x \frac{dy}{\sqrt{x_c^{a+1} - y^{a+1}}} = \sqrt{\frac{2c_2}{M(a+1)}} (t - t_c).$$

Next, we'll move on to the new integration variable $\xi = y/x_c$ considering that:

$$c_2 = c_1 K^2; \sqrt{\frac{2c_2}{M(\alpha + 1)}} = \frac{Kv_0}{x_c^{\frac{\alpha+1}{2}}}.$$

Then, the second integral of the equation of motion takes the form:

$$\int_1^{\frac{x}{x_c}} \frac{d\xi}{\sqrt{1 - \xi^{\alpha+1}}} = \frac{Kv_0}{x_c} (t - t_c).$$

Its left part is an integral representation of the Ateb-sine [20, 23, 24]. Therefore, the analytical solution of the problem at the decompression stage is expressed through this special function and has the form:

$$x(t) = x_c Ca\left(\alpha, 1; \frac{1 + \alpha}{2} \cdot \frac{Kv_0}{x_c} (t - t_c)\right) \tag{9}$$

Calculating the impact force during decompression of bodies is reduced to the use of the formula:

$$P(t) = P_c^* \left[Ca\left(\alpha, 1; \frac{1 + \alpha}{2} \cdot \frac{Kv_0}{x_c} (t - t_c)\right) \right]^\alpha \tag{10}$$

where: $P_c^* = c_2 x_c^\alpha = c_2 \left(\frac{Mv_0^2}{2} \cdot \frac{\alpha + 1}{c_1} \right)^{\frac{1}{\alpha+1}}.$

If $t = t_c$, the force of dynamic interaction of bodies has a height jump:

$$\Delta P = P_c - P_c^* = (c_1 - c_2)x_c^\alpha = 2(\Delta c)x_c^\alpha.$$

The process of decompression ends when:

$$t = t_y = t_c + \frac{x_c}{Kv_0} I = \left(1 + \frac{1}{K}\right) \frac{x_c}{v_0} I. \tag{11}$$

This is the formula of impact duration.

RESULTS AND DISCUSSION

Using the presented theory, its numerical implementation was carried out. For calculations $x(t)$ and $P(t)$ according to formulas (3), (6) and (9), (10) it is necessary to have the values of the periodic Ateb-functions. If we limit ourselves to approximate results, then these values are quite simple to obtain using their approximations in the first quarter of the period $\eta \in [0; I]$:

$$\begin{aligned} Sa\left(\alpha, 1; \frac{1 + \alpha}{2} \eta\right) &\approx \sin\left(\frac{\pi\eta}{2I} + B \sin \frac{\pi\eta}{I} + C \sin \frac{2\pi\eta}{I}\right); \\ Ca\left(\alpha, 1; \frac{1 + \alpha}{2} \eta\right) &\approx \cos\left(\frac{\pi\eta}{2I} - B \sin \frac{\pi\eta}{I} + C \sin \frac{2\pi\eta}{I}\right). \end{aligned} \tag{12}$$

Here:

$$\begin{aligned} B &= \arcsin\left[Sa\left(\alpha, 1; \frac{1 + \alpha}{2} \cdot \frac{I}{2}\right) \right] - \frac{\pi}{4}; \\ C &= \arcsin\left[Sa\left(\alpha, 1; \frac{1 + \alpha}{2} \cdot \frac{I}{4}\right) \right] - \frac{\pi}{8} - B \sin \frac{\pi}{4}; \end{aligned}$$

where: I is determined according to the formula (5).

Let's consider the examples.

Example 1

We take the same input data as in the paper [14], where: $M = 0.1 \text{ kg}$; $E_1 = 0.8 \cdot 10^7 \text{ Pa}$; $\nu_1 = 0.5$; $E_2 = 2750 \cdot 10^7 \text{ Pa}$; $\nu_2 = 0.15$; $c = 2.1873 \cdot 10^6 \text{ Nm}^{-3/2}$; $K = 0.73$; $a = 2/3$. For these data $c_1 = 2.8538 \cdot 10^6 \text{ Nm}^{-3/2}$; $c_2 = 1.5208 \cdot 10^6 \text{ Nm}^{-3/2}$. The calculated values of the characteristics when a rubber ball hits a concrete half-space with different speeds are given in Table 1.

Table 1. Impact characteristics at various v_0 ($K = 0,73$)

$v_0, \text{ m/s}$	$10^3 x_c, \text{ m}$	$P_c, \text{ N}$	$P_c^*, \text{ N}$	$10^3 t_c, \text{ s}$	$10^3 t_y, \text{ s}$
1	1.139	109.70	58.46	1.676	3.972
2	1.983	252.00	134.30	1.459	3.458
3	2.743	409.98	218.48	1.346	3.190
4	3.453	579.05	308.59	1.270	3.010
5	4.128	756.89	403.36	1.215	2.879

Note: Using formulas (4) and (11), when determining t_c and t_y , in the formula (5) applied: $G(0,4) \approx 2,21825$; $G(0,9) \approx 1,06867$. Thus, $I \approx 1,47164$.

To compare the results, we use graphs $P(t)$ and $x(t)$ (Fig. 1), taken from the paper [14]. The results presented in Table 1 are completely consistent with those on the graphs (Fig. 1), because they coincide with them as extreme points.

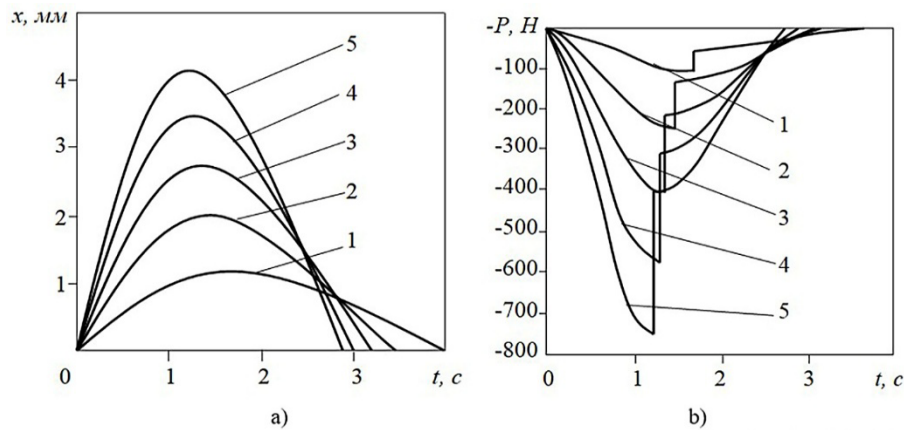


Figure 1. Dependencies of deformation (a) and contact force (b) on time at $v_0 = 1(1), 2(2), 3(3), 4(4), 5(5) \text{ m/s}$

To evaluate the effect of positional friction on the impact process, Table 2 shows the results of calculations according to the classical theory when $K = 1$; $c_1 = c_2 = c$; $P_c = P_c^*$; $t_y = 2t_c$.

Table 2. Impact characteristics at various v_0 ($K = 1$)

$v_0, \text{ m/s}$	$10^3 x_c, \text{ m}$	$P_c = P_c^*, \text{ N}$	$10^3 t_y, \text{ s}$
1	1.267	98.64	3.729
2	2.206	226.63	3.246
3	3.051	368.61	2.993
4	3.841	520.69	2.826
5	4.592	680.57	2.703

By comparing the results in Table 1 and Table 2, it was established that considering positional friction leads to a decrease in the maximum compression of bodies, an increase in the maximum impact force and the compression process over time.

To calculate $x(t)$ and $P(t)$ according to formulas (3), (6) and (9), (10) it is necessary to have values of periodic Ateb-functions. They can be obtained according to formulas (12), in which it is necessary to introduce: $a = 3/2$; $B = -0.02613$; $C = -0.00207$; $I = 1.47164$.

Information about the accuracy of approximations (12) is given in Table 3, where along with the conditionally accurate ones (up to 10^{-4}), the approximate values of the periodic Ateb-functions in the first quarter of their period are given in brackets.

Table 3. Accurate and approximate values of Ateb-functions

η/I	$10 \cdot Sa(3/2, 1, 5/4\eta)$	$10 \cdot Ca(3/2, 1, 5/4\eta)$
0.0	0.000 (0.000)	10.000 (10.000)
0.1	1.470 (1.472)	9.865 (9.866)
0.2	2.924 (2.945)	9.466 (9.468)
0.3	4.334 (4.333)	8.818 (8.821)
0.4	5.667 (5.665)	7.947 (7.949)
0.5	6.884 (6.884)	6.884 (6.884)
0.6	7.947 (7.949)	5.667 (5.665)
0.7	8.818 (8.821)	4.334 (4.333)
0.8	9.466 (9.468)	2.924 (2.925)
0.9	9.865 (9.866)	1.470 (1.472)
1.0	10.000 (10.000)	0.000 (0.000)

Note: Approximations (12) ensure accuracy to three significant digits after the decimal point.

It is not difficult to make sure that the data given in Table 3 correspond to the graph $x(t)$ s (Fig. 1).

Example 2

Keeping the previous characteristics of the materials and the mass of the body hitting the half-space, in example 1 we will change only the contact surface of the second order to the contact surface of the fourth order $z_1 = Ar^4$ where $A > 0$ and r is a radial coordinate (Fig. 2).

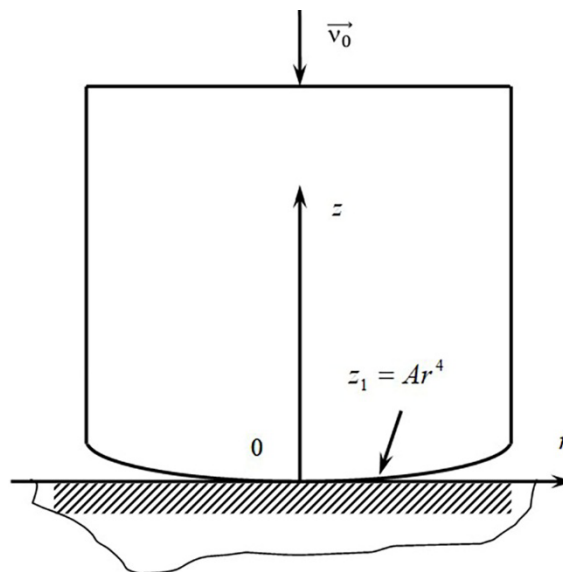


Figure 2. Scheme of contact interaction of bodies bounded by smooth surfaces

Using the solution of I.Ya. Steyerman [22], we obtain the formula for calculating the stiffness of the system:

$$C = \frac{8}{5(Q_1+Q_2)} \left(\frac{3}{8A} \right)^{1/4},$$

where: $Q_1 = \frac{1-v_1^2}{E_1}, Q_2 = \frac{1-v_2^2}{E_2}$.

The force of interaction of bodies P also remains a power function of the convergence of the centers of mass of bodies

$$P = C \cdot x^\alpha \tag{13}$$

where: $\alpha = 5/4$.

But taking into account the positional friction, as before, at the stage of compression it is necessary to replace c with c_1 , and at the stage of compression – c with c_2 .

Let's consider the geometric parameter to be $A = 10^4 \text{ m}^3$, and the impact of the bodies to occur at the initial speed $v_0 = 5 \text{ m/s}$. With such numerical data: $c = 1.3350 \cdot 10^6 \text{ Nm}^{-5/4}$; $c_1 = 1.7418 \cdot 10^6 \text{ Nm}^{-5/4}$; $c_2 = 0.9282 \cdot 10^6 \text{ Nm}^{-5/4}$. The calculated impact parameters are: $x_c = 0.002666 \text{ m}$; $P_c = 1055.05 \text{ N}$; $P_c^* = 562.23 \text{ N}$; $t_y = 0.001916 \text{ s}$. They are significantly different from those given in Table 1 when $v_0 = 5 \text{ m/s}$. Therefore, the geometry of the boundary surfaces in the contact area can significantly affect the impact characteristics.

To get $x(t)$ and $P(t)$ when $\alpha = 5/4$, we need to know the value $Sa\left(\frac{5}{4}, 1; \frac{9}{8} \cdot \frac{v_0 t}{x_c}\right)$ and $Ca\left(\frac{5}{4}, 1; \frac{9}{8} \cdot \frac{v_0 t}{x_c}\right)$.

They can be approximately calculated using formulas (12), but we need to apply: $B = -0.01350$; $C = -0.00139$; $I = 1.51640$. The value I was calculated according to the formula (5) taking into account that $G(4/9) \approx 1.99289$ and $G(17/18) \approx 1.03529$.

Information about the accuracy of such trigonometric approximation is given in Table 4, where along with the exact values, the results of using formulas (12) are given in brackets.

Table 4. Exact and approximate values of special functions

η/I	$10 \cdot Sa(5/4, 1, 9/8\eta)$	$10 \cdot Ca(5/4, 1, 9/8\eta)$
0.0	0.000 (0.000)	10.000 (10.000)
0.1	1.513 (1.512)	9.871 (9.872)
0.2	3.001 (3.002)	9.488 (9.490)
0.3	4.431 (4.431)	8.864 (8.866)
0.4	5.768 (5.767)	8.017 (8.019)
0.5	6.975 (6.975)	6.975 (6.975)
0.6	8.017 (8.019)	5.768 (5.767)
0.7	8.864 (8.866)	4.431 (4.431)
0.8	9.488 (9.490)	3.001 (3.002)
0.9	9.871 (9.872)	1.513 (1.512)
1.0	10.000 (10.000)	0.000 (0.000)

As we can see, the differences between exact and approximate values of the Ateb- functions in this table are not significant.

Example 3

By analogy with studies [21], consider the collinear impact of bodies, when there is a special point on the boundary surface of one of them, in which there is an infinite curvature of the surface. At the same time, we additionally take into account positional friction, which corresponds to the specified

coefficient of speed recovery. The equation of the surface with a singular point has the form $z_1 = Ar^{3/2}$ where $A > 0$, r – radial coordinate (Fig.3). To calculate the stiffness of the system, we have the formula:

$$C \approx \frac{0.81180}{A^{2/3}(Q_1+Q_2)}$$

Impact force, as in formula (13), remains a power function x , but now $\alpha = 5/3$.

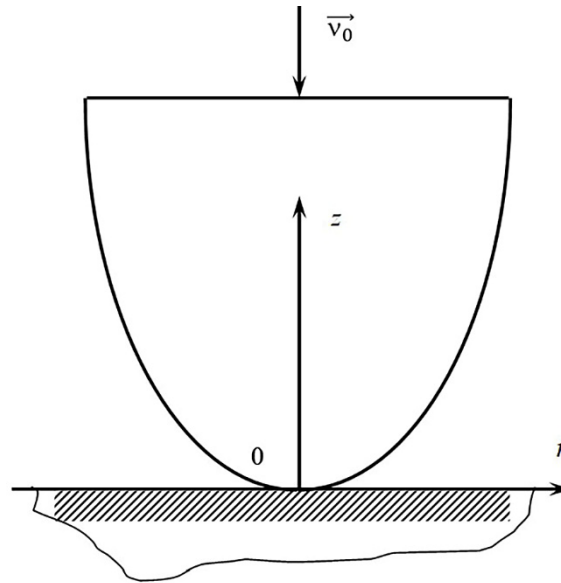


Figure 3. Contact of bodies with a singular point on the surface

For calculations, we take the same input data as in the previous examples, setting $A = 5 \text{ m}^{-1/2}$; $K = 0,73$. These data correspond to: $c = 2.9603 \cdot 10^6 \text{ Nm}^{-5/3}$; $c_1 = 3.8624 \cdot 10^6 \text{ Nm}^{-5/3}$; $c_2 = 2.0582 \cdot 10^6 \text{ Nm}^{-5/3}$. At the initial impact speed $v_0 = 5 \text{ m/s}$ we get: $x_c = 5.3212 \cdot 10^{-3} \text{ m}$; $P_c = 626.4273 \text{ N}$; $P_c^* = 333.8113 \text{ N}$; $t_y = 3.647 \cdot 10^{-3} \text{ s}$. When calculating t_y according to the formula (11) we took into consideration that in the formula (14) $I = 1.445927$. In Example 3, value x_c is bigger, and values P_c and P_c^* are than in the previous examples, which is a consequence of reducing the stiffness of the system due to the presence of a singular point in the area of contact of bodies. For calculation $x(t)$ i $P(t)$, it's necessary to calculate the value $Sa\left(\frac{5}{3}, 1; \frac{4}{3} \cdot \frac{v_0 t}{x_c}\right)$ and $Ca\left(\frac{5}{3}, 1; \frac{4}{3} \cdot \frac{v_0 t}{x_c}\right)$. For this, we can use formulas (12) where now $B = -0.02613$; $C = -0.00207$; $I = 1.47164$.

To obtain information about the errors of formulas (12), the approximate values were compared with the accurate values obtained in [21] by numerical integration of the impact equation on a computer. The results of the comparison of the approximate values with the accurate ones are given in Table 5.

Table 5. Accurate and approximate values of the ratio $x(t)/x_c$

$v_0 t / x_c$	Value $x(t)/x_c$ according to		$v_0 t / x_c$	value $x(t)/x_c$ according to	
	[21]	f. (3), (12)		[21]	f. (3), (12)
0.3615	0.3582	0.3582	1.0845	0.9149	0.9153
0.7230	0.6826	0.6826	1.4459	1.0000	1.0000

The analysis of data in Table 5 proved a good consistency of the calculation results of $x(t)$ by the both methods. The calculations according to formula (12) confirmed the high accuracy of the approximations. Therefore, the numerical implementation of formulas (3), (6) and (9), (10) does not cause complications.

The developed dissipative impact model is quite general. It allows to make calculations of collinear impacts of solid bodies, bounded by various surfaces. The inclusion of positional friction does not change the system's nonlinearity index. It remains the same as in the case of perfectly elastic impacts, but in the dissipative model, the processes of dynamic compression and decompression of the bodies differ quantitatively due to the varying stiffness of the system at these stages.

Since the velocity restitution coefficient is specified as an input parameter in the proposed model, its dependence on the impact velocity, which is the focus of the calculation, is accounted for a priori. As a result, the proposed theory avoids the drawback of known dissipative impact models, in which the velocity restitution coefficient is not predefined but is calculated based on the determined stiffness characteristics of the system during the dynamic compression and decompression phases of the bodies [27]. In such models, the restitution coefficient does not depend on the impact velocity, which contradicts well-established experimental data. Thus, by altering the problem's formulation, this model eliminates that shortcoming, thereby improving its accuracy and adequacy.

CONCLUSIONS

Based on the results of calculations and analyses, the following conclusions were presented:

1. Closed-form analytical solutions for impact equations during the compression and decompression phases of bodies, considering dry positional friction, have been constructed using Ateb-functions.
2. Compact trigonometric approximations of periodic Ateb-functions have been proposed, significantly simplifying the numerical implementation of the analytical solutions.
3. It has been established that the inclusion of positional friction has a significant impact on the calculated impact parameters. It reduces

the maximum approach of the bodies' centers of mass, increases the maximum impact force, and extends the duration of the dynamic interaction. These parameters also depend significantly on the shape of the bodies' boundary surfaces in the contact area.

4. Modifications were made to the formulation of the dissipative impact problem, where the velocity restitution coefficient is now treated as an input parameter for the calculations. The dependence of the restitution coefficient on the initial impact velocity must also be considered.

REFERENCES

1. Yaseena M., Kumara M., Rawat S.K. Assisting and opposing flow of a MHD hybrid nanofluid flow past a permeable moving surface with heat source/sink and thermal radiation. *Partial Differential Equations in Applied Mathematics*, 2021; 4, 100168. <https://doi.org/10.1016/j.padiff.2021.100168>
2. Olshanskii V., Olshanskii A., Kharchenko S., Kharchenko F. About motion of grain mixture of variable porosity in the cylindrical sieve of vibrocentrifuge. *Teka Commission of Motorization and Power Industry in Agriculture*, 2016; 16(3), 31–34.
3. Jagusiak-Kocik M., Bohomolov O., Hurskyi P., Bredykhin V., Lukyanov I., Shchur T., Dzhidzhora O. Optimizing the separation process of difficult to separate wheat and barley grain mixtures using vibrofriction technology. *CzOTO* 2024; 6(1): 360–370, <https://doi.org/10.2478/czoto-202-0038>
4. Bredykhin V., Tikunov S., Slipchenko M., Alfyorov O., Bogomolov A., Shchur T., Kocira S., Kiczorowski P., Paslavskyy R. Improving efficiency of corn seed separation and calibration process. *Agricultural Engineering*, 2023; 27(1): 241–253. <https://doi.org/10.2478/agriceng-2023-0018>
5. Karaiev O., Bondarenko L., Halko S., Miroshnyk O., Vershkov O., Karaieva T., Shchur T., Findura P., Pristavka M. Mathematical modelling of the fruit-stone culture seeds calibration process using flat sieves. *Acta Technologica Agriculturae*, 2021; 24(3): 119–123. <https://doi.org/10.2478/ata-2021-0020>
6. Wang P., Deng X., Jiang S. Global warming grain production and its efficiency: Case study of major grain production region. *Ecological Indicators*, 2019; 105: 563–570. <https://doi.org/10.1016/j.ecolind.2018.05.022>
7. Olshanskyi V.P. Pro udar viazko-pruzhnoho tila ob zhorstku pereshkodu. *Visnyk NTU 'KhPI', Ser.: Dynamika i mitsnist mashyn*, 2018; 38(1314): 37–41.

8. Olshanskyi V.P. Pro udar viazko-pruzhnoho tila ob zhorstku pereshkodu. *Visnyk NTU 'KhPI', Ser.: Matematychno modeliuвання v tekhnitsi ta tekhnolohiiakh*, 2018; 27(1303): 73–78.
9. Brahinets M.V., Dmytriv V.T., Khmelovskiy V.S., Bohomolov O.V., Bohomolov O.O. Modeliuвання protsesu separatsii nasinnia ripaku separatorom udarnoi dii. *Tekhnika ta Enerhetyka. Zhurnal naukovykh doslidzhen silskohospodarskoho vyrobnytstva*. Kyiv, 2020; 11(2): 157–164.
10. Bogomolov A.V. Separatsiya trudnorazdelimiyh syipuchih smesey (nauchnoe obosnovanie energoberegayuschiy protsessov i oborudovaniya). *Monografiya. HNTUSG*, 2013; 296.
11. Bohomolov O.V., Brahinets M.V., Mazunov A.R., Naumenko E.M., Bohomolov O.O., Bohomolova V.P. Udoshkonalennia konstrukttsii hravitatsiinoho bahatoiarusnoho udarnoho separatora. *Visnyk KhNTUSH*, 2019; 207: 75–81.
12. Havrylenko Y., Kholodniak Y., Halko S., Vershkov O., Miroshnyk O., Suprun O., Dereza O., Shchur T., Śrutek M. Representation of a monotone curve by a contour with regular change in curvature. *Entropy*. 2021; 23(7): 923. <https://doi.org/10.3390/e23070923>
13. Olshanskyi V.P., Olshanskyi S.V. Uzahalnena zadacha mekhanichnoho udaru v teorii Hertsa. *Vibratsii v Tekhnitsi ta Tekhnolohiiakh*, 2018; 4(91): 70–75.
14. Bredykhin V., Shchur T., Kis-Korkishchenko L., Denisenko S., Ivashchenko S., Marczuk A., Dzhydzhora O., Kubon M. Determination of ways of improving the process of separation of seed materials on the working surface of the pneumatic sorting table. *Agricultural Engineeringthis*, 2024; 28: 51–71. <https://doi.org/10.2478/agriceng-2024-0005>
15. Fu G. An extension of Hertz's theory in contact mechanics. *Journal of Applied Mechanics*, 2007; 74(2): 373–374. <https://doi.org/10.1115/1.2188017>
16. Gendelman O., Vakakis A.F. Transition from localization to nonlocalization in strongly nonlinear damped oscillators. *Chaos, Solitons and Fractals*, 2000; 11(10): 1535–1542. [https://doi.org/10.1016/S0960-0779\(99\)00076-4](https://doi.org/10.1016/S0960-0779(99)00076-4)
17. Cveticanin L., Pogany T. Oscillator with a sum of noninteger – order nonlinearities. *Journal of Applied Mathematics*, 2012, 649050. <https://doi.org/10.1155/2012/649050>
18. Pukach P.Ya., Kuzio I.V. Resonance phenomena in quasi-zero stiffness vibration isolation systems. *Naukovyi Visnyk Nationalnogo Hirnychoho Universytety*, 2015; 3: 62–67.
19. Pukach P. Investigation of bending vibrations Voigt-Kelvin bars with regard for nonlinear resistance force. *Journal of Mathematical Sciences*, 2016; 215(1): 71–78. <https://doi.org/10.1007/s10958-016-2823-0>
20. Olshanskyi V.P., Olshanskyi S.V. Ateb-synus u rozviazku zadachi Hertsa pry udari. *Visnyk NTU 'KhPI' Ser. Matematychno modeliuвання v tekhnitsi ta tekhnolohiiakh*. Kharkiv, 2018; 3(1279): 98–193.
21. Olshanskii V., Spolnik O., Slipchenko M., Znaidiuk V. Modeling the elastic impact of a body with a special point at its surface. *Eastern-European Journal of Enterprise Technologies*, 2019; 1/7(97): 25–32. <https://doi.org/10.15587/1729-4061.2019.155854>
22. Havrylenko Y., Kholodniak Y., Halko S., Vershkov O., Bondarenko L., Suprun O., Miroshnyk O Shchur T., Śrutek M., Gackowska M. Interpolation with specified error of a point series belonging to a monotone curve. *Entropy*. 2021; 23(5): 493. doi.org/10.3390/e23050493
23. Olshanskyi V.P. Pro rukh ostsylatora zi stepenevoiu kharakterystykoiu pruzhnosti. *Vibratsii i Tekhnitsi ta Tekhnolohiiakh*, 2017; 3(68): 34–40.
24. Olshanskyi V.P., Bohomolov O.V., Bohomolov O.O. Pro peretvorennia udarom zadempfovanoi mekhanichnoi systemy v ostsylator. *Suchasni napriamy tekhnolohii ta mekhanizatsii protsesiv pererobnykh ta kharchovykh vyrobnytstv*. *Visnyk KhNTUSH*, 2018; 194: 18–31.
25. Yang B. Machine learning-based evolution model and the simulation of a profit model of agricultural products logistics financing. *Neural Computing and Applications*, 2019; 31(9), 4733–4759. <https://doi.org/10.1007/s00521-019-04072-5>
26. Setooden A., Azizi A. Bending and free vibration analyses of rectangular laminated composite plates resting on elastic foundation using a refined shear deformation theory. *Iranian Journal of Materials Forming*, 2015; 2(2): 1–13. <https://doi.org/10.22099/ijmf.2015.3236>
27. Du J., Wang S., He C., Zhou B., Ruan Y.-L., Shou H. Identification of regulatory networks and hub genes controlling soybean seed set and size using RNA sequencing analysis. *Journal of Experimental Botany*, 2017; 68(8): 1955–1972. <https://doi.org/10.1093/jxb/erw460>